

## Article

# Increasing the Effectiveness of Active Learning: Introducing Artificial Data Generation in Active Learning for Land Use/Land Cover Classification

Joao Fonseca <sup>1,\*</sup>, Georgios Douzas <sup>1</sup>, Fernando Bacao <sup>1</sup>

<sup>1</sup> NOVA Information Management School (NOVA IMS), Universidade Nova de Lisboa, Campus de Campolide, 1070-312 Lisboa, Portugal; gdouzas@novaims.unl.pt (G.D.); bacao@novaims.unl.pt (F.B.)

\* Correspondence: jpfonseca@novaims.unl.pt (J.F.)

\* Correspondence: jpfonseca@novaims.unl.pt

**1 Abstract:** In remote sensing, Active Learning (AL) has become an important technique to collect informative ground truth data “on-demand” for supervised classification tasks. In spite of its effectiveness, it is still significantly reliant on user interaction, which makes it both expensive and time consuming to implement. Most of the current literature focuses on the optimization of AL by modifying the selection criteria and the classifiers used. Although improvements in these areas will result in more effective data collection, the use of artificial data sources to reduce human-computer interaction remains unexplored. In this paper, we introduce a new component to the typical AL framework, the data generator, a source of artificial data to reduce the amount of user-labeled data required in AL. The implementation of the proposed AL framework is done using Geometric SMOTE as data generator. We compare the new AL framework to the original one using similar acquisition functions and classifiers over three AL-specific performance metrics in seven benchmark datasets. We show that this modification of the AL framework significantly reduces cost and time requirements for a successful AL implementation in all of the datasets used in the experiment.

**15 Keywords:** Active Learning; Artificial Data Generation; Land Use/Land Cover Classification;  
16 Oversampling; SMOTE

## 17 1. Introduction

18 The technological development of air and spaceborne sensors, as well as the increasing number of remote sensing missions have allowed the continuous collection  
19 of large amounts of high quality remotely sensed data. This data is often composed of multi and hyper spectral satellite imagery, essential for numerous applications, such  
20 as Land Use/Land Cover (LULC) change detection, ecosystem management [1], agricultural management [2], water resource management [3], forest management, and  
21 urban monitoring [4]. Despite LULC maps being essential for most of these applications,  
22 their production is still a challenging task [5,6]. They can be updated using one of the  
23 following strategies:

- 24 1. Photo-interpretation. This approach consists of evaluating a patch’s LULC class by  
25 a human operator based on orthophoto and satellite image interpretation [7]. This  
26 method guarantees a decent level of accuracy, as it is dependent on the interpreter’s  
27 expertise and human error. Typically, it is an expensive, time-consuming task that  
28 requires the expertise of a photo-interpreter. This task is also frequently applied to  
29 obtain ground-truth labels for training and/or validating Machine Learning (ML)  
30 algorithms for related tasks [8,9].

**Citation:** Fonseca, J.; Douzas, G.; Bacao, F. Increasing the Effectiveness of Active Learning: Introducing Artificial Data Generation in Active Learning for Land Use/Land Cover Classification. *Remote Sens.* **2021**, *1*, 0.  
<https://doi.org/>

Received:

Accepted:

Published:

**Publisher’s Note:** MDPI stays neutral with regard to jurisdictional claims in published maps and institutional affiliations.

**Copyright:** © 2021 by the authors. Submitted to *Remote Sens.* for possible open access publication under the terms and conditions of the Creative Commons Attribution (CC BY) license (<https://creativecommons.org/licenses/by/4.0/>).

- 35 2. Automated mapping. This approach is based on the usage of a ML method or a  
36 combination of methods in order to obtain an updated LULC map. The develop-  
37 ment of a reliable automated method is still a challenge among the ML and remote  
38 sensing community, since the effectiveness of existing methods varies across applica-  
39 tions and geographical areas [5]. Typically, this method requires the existence of  
40 ground-truth data, which is frequently outdated or nonexistent for the required  
41 time frame [1]. On the other hand, employing a ML method provides readily  
42 available and relatively inexpensive LULC maps. The increasing quality of state-of-  
43 the-art classification methods have motivated the application and adaptation of  
44 these methods in this domain [10].
- 45 3. Hybrid approaches. These approaches employ photo-interpreted data to augment  
46 the training dataset and improve the quality of automated mapping [11]. It at-  
47 tempts to accelerate the photo-interpretation process by selecting a smaller sample  
48 of the study area to be interpreted. The goal is to minimize the inaccuracies found  
49 in the LULC map by supplying high-quality ground-truth data to the automated  
50 method. The final (photo-interpreted) dataset consists of only the most informa-  
51 tive samples, *i.e.*, patches that are typically difficult to classify for a traditional  
52 automated mapping method [12].

53 The latter method is best known as AL. It is especially useful whenever there is a  
54 shortage or even absence of ground-truth data and/or the mapping region does not  
55 contain updated LULC maps [13]. In a context of limited sample-collection budget,  
56 the collection of the most informative samples capable of optimally increasing the  
57 classification accuracy of a LULC map is of particular interest [13]. AL attempts to  
58 minimize the human-computer interaction involved in photo-interpretation by selecting  
59 the data points to include in the annotation process. These data points are selected  
60 based on an uncertainty measure and represent the points close to the decision borders.  
61 Afterwards, they are passed on for photo-interpretation and added to the training dataset,  
62 while the points with the lowest uncertainty values are ignored for photo-interpretation  
63 and classification. This process is repeated until a convergence criterion is reached [14].

64 The relevant work developed within AL is described in detail in Section 2. This  
65 paper attempts to address some of the challenges found in AL, mainly inherited from  
66 automated and photo-interpreted mapping: mapping inaccuracies and time consuming  
67 human-computer interactions. These challenges have different sources:

- 68 1. Human error. The involvement of photo-interpreters in the data labeling step  
69 carries an additional risk to the creation of LULC patches. The minimum mapping  
70 unit being considered, as well as the quality of the orthophotos and satellite images  
71 being used, are some of the factors that may lead to the overlooking of small-area  
72 LULC patches and label-noisy training data [15].
- 73 2. High-dimensional datasets. Although the amount of bands (*i.e.*, features) present in  
74 multi and hyper spectral images contain useful information for automated classifi-  
75 cation, they also introduce an increased level of complexity and redundancy in the  
76 classification step [16]. These datasets are often prone to the Hughes phenomenon,  
77 also known as the curse of dimensionality.
- 78 3. Class separability. Producing an LULC map considering classes with similar  
79 spectral signatures makes them difficult to separate [17]. A lower pixel resolution  
80 of the satellite images may also imply mixed-class pixels, which may lead to both  
81 lower class separability as well as higher risk of human error.
- 82 4. Existence of rare land cover classes. The varying morphologies of different geo-  
83 graphical regions naturally implies an uneven distribution of land cover classes [18].  
84 This is particularly relevant in the context of AL since the data selection method  
85 is based on a given uncertainty measure over data points whose class label is  
86 unknown. Consequently, AL's iterative process of data selection may disregard  
87 wrongly classified land cover areas belonging to a minority class.

88 Research developed in the field of AL typically focus on the reduction of human  
89 error by minimizing the human interaction with the process through the development  
90 of more efficient classifiers and selection criteria within the generally accepted AL  
91 framework. Concurrently, the problem of rare land cover classes is rarely addressed.  
92 This is a frequent problem in the ML community, known as the Imbalanced Learning  
93 problem. This problem exists whenever there is an uneven between-class distribution in  
94 the dataset [19]. Specifically, most classifiers are optimized and evaluated using accuracy-  
95 like metrics, which are designed to work primarily with balanced datasets. Consequently,  
96 these metrics tend to introduce a bias towards the majority class by attributing an  
97 importance to each class proportional to its relative frequency [10]. As an example, such a  
98 classifier could achieve an overall accuracy of 99% on a binary dataset where the minority  
99 class represents 1% of the overall dataset and still be useless. A number of methods  
100 have been developed to deal with this problem. They can be categorized into three  
101 different types of approaches [20,21]. Cost-sensitive solutions perform changes to the  
102 cost matrix in the learning phase. Algorithmic level solutions modify specific classifiers  
103 to reinforce learning on minority classes. Resampling solutions modify the training data  
104 by removing majority samples and/or generating artificial minority samples. The latter  
105 is independent from the context and can be used alongside any classifier. Since we are  
106 interested in the introduction of artificial data generation in AL, we will analyze the  
107 state-of-the-art on resampling techniques (specifically oversampling) in Section 3.

108 In this paper, we propose a novel AL framework to address two limitations com-  
109 monly found in the literature: minimize human-computer interaction and reduce the  
110 class imbalance bias. This is done with the introduction of an additional component  
111 in the iterative AL procedure (the generator) that is used to generate artificial data to  
112 both balance and augment the training dataset. The introduction of this component  
113 is expected to reduce the number of iterations required until the classifier reaches a  
114 satisfactory performance.

115 This paper is organized as follows: Section 1 explains the problem and its context,  
116 Sections 2 and 3 describe the state of the art in AL and Oversampling techniques, Section  
117 4 explains the proposed method, Section 5 covers the datasets, evaluation metrics, ML  
118 classifiers and experimental procedure, Section 6 presents the experiment's results and  
119 discussion and Section 7 presents the conclusions drawn from our findings.

## 120 2. Active Learning Approaches

121 As the amount of unlabeled data increases, the interest and practical usefulness of  
122 AL follows that trend [22]. AL is used as the general definition of frameworks aiming to  
123 train a learning system in multiple steps, where a set of new data points are chosen and  
124 added to the training dataset each time [11]. Typically, an AL framework is composed of  
125 the following elements [11,13,23]:

- 127 1. Unlabeled dataset. Consists of the original data source (or a sample thereof). It  
128 is used in combination with the chooser and the selection criterion to expand the  
129 training dataset in regions where the classification uncertainty is higher. Therefore,  
130 the unlabeled dataset is used for both producing the initial training dataset by  
131 selecting a set of instances for the supervisor to annotate (discussed in point 3) and  
132 calculating the uncertainty map to augment the training dataset.
- 133 2. Supervisor. A human annotator (or team of human annotators) to which the  
134 uncertainty map is presented to. The supervisor is responsible for annotating  
135 unlabeled instances to be added to the augmented dataset. In remote sensing,  
136 the supervisor is typically a photo-interpreter, as is the case in [24]. Some of the  
137 research also refers to the supervisor as the *oracle* [11,25–27].
- 138 3. Initial training dataset. It is a small, labeled sample of the original data source used  
139 to initiate the first AL iteration. The size of the initial training sample normally  
140 varies between no instances at all and 10% of the unlabeled dataset [28].

- 141 4. Current and expanded training dataset. It is the concatenation of the initial training  
 142 dataset and the datasets labeled by the supervisor in past iterations (discussed in  
 143 point 2).  
 144 5. Chooser (classifier). Produces the class probabilities for each unlabeled instance.  
 145 6. Selection criterion. It quantifies the chooser's uncertainty level for each instance  
 146 belonging to the unlabeled dataset. It is typically based on the class probabilities  
 147 assigned by the chooser. In some situations, the chooser and the selection criterion  
 148 are grouped together under the concept *acquisition function* [11] or *query function* [13].  
 149 Some of the literature refers to the selection criterion by using the concept *sampling  
 150 scheme* [12].

151 Figure 1 schematizes the steps involved in a complete AL iteration. For a better  
 152 context within the remote sensing domain, the prediction output can be identified as  
 153 the LULC map. This framework starts by collecting unlabeled data from the original  
 154 data source. It is used to generate a random initial training sample and is labeled by  
 155 the supervisor. In practical applications, the supervisor is frequently a group of photo-  
 156 interpreters [22]. The chooser is trained on the resulting dataset and is used to predict the  
 157 class probabilities on the unlabeled dataset. The class probabilities are fed into a selection  
 158 criterion to estimate the prediction's uncertainty, out of which the instances with the  
 159 highest uncertainty will be selected. This calculation is motivated by the absence of  
 160 labels in the uncertainty dataset. Therefore, it is impossible to estimate the prediction's  
 161 accuracy in the unlabeled dataset in a real case scenario. The iteration is completed when  
 162 the selected points are tagged by the supervisor and added to the training dataset (*i.e.*,  
 163 the augmented dataset).

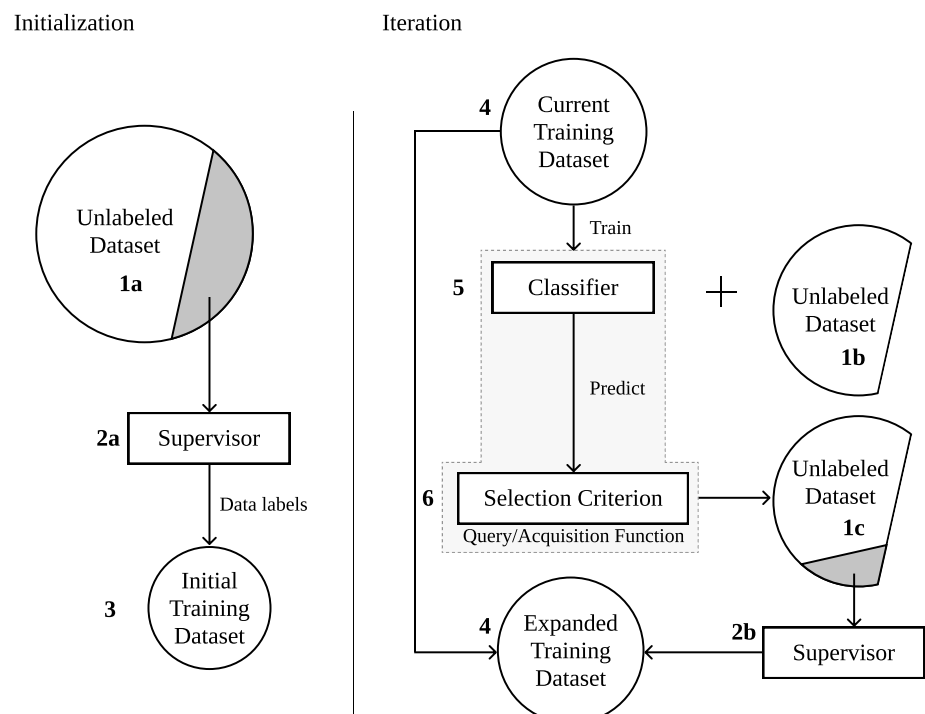


**Figure 1.** Diagram depicting the typical AL framework.

164 A common challenge found in AL tasks is ensuring the consistency of AL over  
 165 different initializations [22]. There are two factors involved in this phenomenon. On one  
 166 hand, the implementation of the same method over different initializations may result in  
 167 significantly different initial training samples, amounts to varying accuracy curves. On  
 168 the other hand, the lack of a robust selection criterion and/or classifier may also result in

169 inconsistencies across AL experiments with different initializations. This phenomenon  
170 was observed and documented in a LULC classification context in [29].

171 The classification method plays a central role in the efficacy of AL. The classifier  
172 used should be able to generalise with a relatively small training dataset. Specifically,  
173 deep learning models are used in image classification due to its capability of producing  
174 high quality predictions. Although, to make such models generalizable the training set  
175 must be large enough, making its suitability for AL applications an open challenge [30–  
176 32]. Some studies in the Remote Sensing domain were developed to address this gap.  
177 In [30,32], the authors propose a deep learning-based AL approach by training the  
178 same Convolutional Neural Network incrementally across iterations and smoothen  
179 the decision boundaries of the model using the Markov Random Field model and a  
180 Best-versus-Second Best labelling approach. This allows the introduction of additional  
181 data variability in the final training dataset. Another study [31] combined transfer  
182 learning, active classification and segmentation techniques for vehicle detection. By  
183 combining different techniques, they were able to produce a classification mechanism  
184 that performed well when the amount of training data is limited.

185 Selecting an efficient selection criterion is particularly important to find the instances  
186 closest to the decision border (*i.e.*, instances difficult to classify) [33]. Therefore, many  
187 AL related studies focus on the design of the query/acquisition function [13].

### 188 2.1. Non-informed selection criteria

189 Only one non-informed (*i.e.*, random) selection criterion was found in the literature.  
190 Random sampling selects unlabeled instances without considering any external informa-  
191 tion produced by the chooser. Since the method for selecting the unlabeled instances is  
192 random, this method disregards the usage of a chooser and is comparatively worse than  
193 any other selection criterion. However, random sampling is still a powerful baseline  
194 method [27].

### 195 2.2. Ensemble-based selection criteria

196 Ensemble disagreement is based on the class predictions of a set of classifiers. The  
197 disagreement between all the predictions for a given instance is a common measure for  
198 uncertainty, although computationally inefficient [11,14]. It is calculated using the set of  
199 classifications over a single instance, given by the number of votes assigned to the most  
200 frequent class [33]. This method was implemented successfully for complex applications  
201 such as deep active learning [11].

202 Multiview [34] consists on the training of multiple independent classifiers using  
203 different views, which correspond to the selection of subsets of features or instances  
204 in the dataset. Therefore, it can be seen as a bootstrap aggregation (bagging) ensemble  
205 disagreement method. It is represented by the maximum disagreement score out of set  
206 of disagreements calculated for each view [33]. A lower value for this metric means a  
207 higher classification uncertainty. Multiview-based maximum disagreement has been  
208 successfully applied to hyper-spectral image classification in [35] and [36].

209 An adapted disagreement criterion for an ensemble of  $k$ -nearest neighbors has been  
210 proposed in [14]. This method employs a  $k$ -nearest neighbors classifier and computes  
211 an instance's classification uncertainty based on the neighbors' class frequency using  
212 the maximum disagreement metric over varying values for  $k$ . As a result, this method is  
213 comparable to computing the dominant class' score over a weighted  $k$ -nearest neighbors  
214 classifier. This method was also used on a multimetric active learning framework [37].

215 Another relevant ensemble-based selection criterion is the binary random forest-  
216 based query model [13]. This method employs a one-versus-one ensemble method  
217 to demonstrate an efficient data selection method using the estimated probability of  
218 each binary random forest and determining the classification uncertainty based on the  
219 probabilities closest to 0.5 (*i.e.*, the least separable pair of classes are used to determine

220 the uncertainty value). However, this study fails to compare the proposed method with  
221 other benchmark methods, such as random sampling.

### 222 2.3. *Entropy-based criteria*

223 A number of contributions have focused on entropy-based querying. The appli-  
224 cation of entropy is common among active deep learning applications [26], where the  
225 training of an ensemble of classifiers is often too expensive.

226 Entropy query-by-bagging (EQB), also defined as maximum entropy [12], is an  
227 ensemble approach of the entropy selection criterion, originally proposed in [38]. This  
228 strategy uses the set of predictions produced by the ensemble classifier to calculate those  
229 many entropy measurements. The estimated uncertainty measure for one instance is  
230 given by the maximum entropy within that set. EQB was observed to be an efficient  
231 selection criterion. Specifically, [33] applied EQB on hyper-spectral remote sensing im-  
232 agery using Support Vector Machines (SVM) and Extreme Learning Machines (ELM) as  
233 choosers, achieving optimal results when combining EQB with ELM. Another study suc-  
234 cessfully implemented this method on an active deep learning application [12]. Another  
235 study improved over this method with a normalized EQB selection criterion [39].

### 236 2.4. *Other relevant criteria*

237 Margin Sampling is a SVM-specific criterion, based on the distance of a given point  
238 to the SVM's decision boundary [33]. This method is less popular than the remaining  
239 methods because it is limited to one type of chooser (SVMs). One extension of this  
240 method is the multiclass level uncertainty [33], calculated by subtracting the instance's  
241 distance to the decision boundaries of the two most probable classes [40].

242 The Mutual Information-based (MI) criterion selects the new training instances  
243 by maximizing the mutual information between the classifier and class labels in order  
244 to select instances from regions that are difficult to classify. Although this method is  
245 commonly used, it is frequently outperformed by the breaking ties selection criterion [41,  
246 42].

247 The breaking ties (BT) selection criterion was originally introduced in [43]. It  
248 consists of the subtraction between the probabilities of the two most likely classes.  
249 Another related method is Modified Breaking Ties scheme (MBT), which aims at finding  
250 the instances containing the largest probabilities for the dominant class [42,44].

251 Another type of selection criteria identified is the loss prediction method [25]. This  
252 method replaces the selection criterion with a predictor whose goal is to estimate the  
253 chooser's loss for a given prediction. This allows the new classifier to estimate the  
254 prediction loss on unlabeled instances and select the ones with the highest predicted  
255 loss.

256 Some of the literature fails to specify the strategy employed, although inferring it is  
257 generally intuitive. For example, [45] successfully used AL to address the imbalanced  
258 learning problem. They employed an ensemble of SVMs as the chooser, as well as  
259 an ensemble-based selection criterion. All of the research found related to this topic  
260 focused on the improvement of AL through modifications on the selection criterion  
261 and classifiers used. None of these publications proposed significant variations to the  
262 original AL framework.

## 263 3. Artificial Data Generation Approaches

264  
265 The generation of artificial data is a common approach to address imbalanced learn-  
266 ing tasks [21], as well as improving the effectiveness of supervised learning tasks [46]. In  
267 recent years some sophisticated data generation approaches were developed. However,  
268 the scope of this work is to propose the integration of a generator within the AL frame-  
269 work. To do this, we will focus on heuristic data generation approaches, specifically,  
270 oversamplers.

271 Heuristic data resampling methods employ local and/or global information to  
 272 generate new, relevant, non-duplicate instances. These methods are most commonly  
 273 used to populate minority classes and balance the between-class distribution of a dataset.  
 274 The Synthetic Minority Oversampling Technique (SMOTE) [47] is a popular heuristic  
 275 oversampling algorithm, proposed in 2002. The simplicity and effectiveness of this  
 276 method contributes to its prevailing popularity. It generates a new instance through  
 277 a linear interpolation of a randomly selected minority-class instance and one of its  
 278 randomly selected  $k$ -nearest neighbors. The implementation of SMOTE for LULC clas-  
 279 sification tasks has been found to improve the quality of the predictors used [48,49].  
 280 Despite its popularity, its drawbacks motivated the development of other oversampling  
 281 methods [50].

282 Geometric SMOTE (G-SMOTE) [50] introduces a modification of the SMOTE al-  
 283 gorithm in the data generation mechanism to produce artificial instances with higher  
 284 variability. Instead of generating artificial data as a linear combination of the parent  
 285 instances, it is done within a deformed, truncated hyper-spheroid. G-SMOTE gener-  
 286 ates an artificial instance  $\vec{z}$  within a hyper-spheroid, formed by selecting a minority  
 287 instance  $\vec{x}$  and one of its nearest neighbors  $\vec{y}$ , as shown in Figure 2. The truncation  
 288 and deformation parameters define the shape of the spheroid's geometry. The method  
 289 also modifies the selection strategy for the  $k$ -nearest neighbors, accepting the generation  
 290 of artificial instances using instances from different classes, as shown in Figure 2d. The  
 291 modification of both selection and generation mechanisms addresses the main draw-  
 292 backs found in SMOTE, the generation of both noisy data (*i.e.*, generate minority class  
 293 instances within majority class regions) and near-duplicate minority class instances [50].  
 294 G-SMOTE has shown superior performance when compared with other oversampling  
 295 methods for LULC classification tasks, regardless of the classifier used [51].

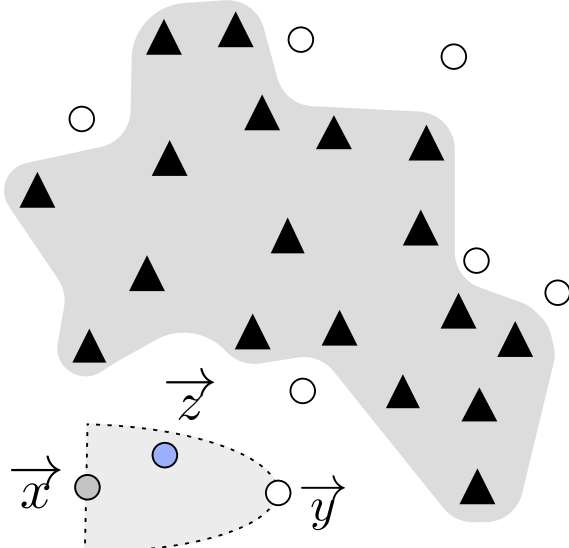


**Figure 2.** Example of G-SMOTE's generation process. G-SMOTE randomly selects instance  $\vec{x}$  and one of its nearest neighbors  $\vec{y}$  to produce instance  $\vec{z}$ .

#### 296 4. Proposed method

297 Within the literature identified, most of the work developed in the AL domain  
 298 revolved around improving the quality of classification algorithms and/or selection  
 299 criteria. Although these methods allow earlier convergence of the AL iterative process,  
 300 the impact of these methods are only observed between iterations. Consequently, none  
 301 of these contributions focused on the definition of decision borders within iterations. The

method proposed in this paper modifies the AL framework by introducing an artificial data generation step within AL's iterative process. We define this component as the generator and is intended to be integrated into the AL framework as shown in Figure 3.

This modification, by using a new source of data to augment the training set, leverages the data annotation work conducted by the human operator. The artificial data that is generated between iterations reduces the amount of labeled data required to reach optimal performance and lower the amount of human labor required to train a classifier to its optimal performance. This process lowers the annotation and overall training costs by translating some of the annotation cost into computational cost.

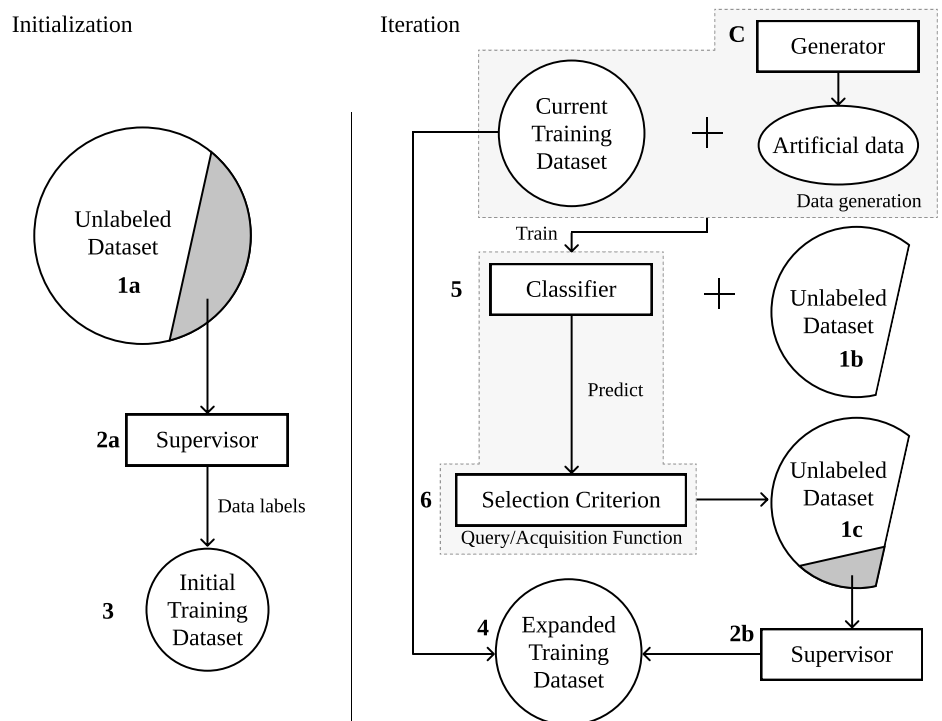


**Figure 3.** Proposed AL framework. This paper's contribution comprises a change in the AL framework through the introduction of a data generation mechanism, represented as the generator (marked with C), which is used to add artificial instances to the training dataset.

This method leverages the capability of artificial data to introduce more data variability into the augmented dataset and facilitate the chooser's training phase with a more consistent definition of the decision boundaries at each iteration. Therefore, any algorithm capable of producing artificial data, be it agnostic or specific to the domain, can be employed. The artificial data is only used to train the classifiers involved in the process and is discarded once the training phase is completed. The remaining steps in the AL framework remain unchanged. This method addresses the limitations found in the previous sections:

- 312 1. The convergence of classification performance should be anticipated with the  
313 clearer definition of the decision boundaries across iterations.
- 314 2. Annotation cost is expected to reduce as the need for labeled instances reduces  
315 along with the early convergence of the classification performance.
- 316 3. The class imbalance bias observed in typical classification tasks, as well as in AL is  
317 mitigated by balancing the class frequencies at each iteration.

326 Although the performance of this method is shown within a LULC classification  
327 context, the proposed framework is independent from the domain. The high dimension-

ability of remotely sensed imagery make its classification particularly challenging when the availability of labeled data is scarce and/or comes at a high cost, being subjected to the curse of dimensionality. Consequently, it is a relevant and appropriate domain to test this method.

## 5. Methodology

In this section we describe the datasets, evaluation metrics, oversampler, classifiers, software used and the procedure developed. We demonstrate the proposed method's efficiency over 7 datasets, sampled from publicly available, well-known remote sensing hyperspectral scenes frequently found in remote sensing literature. The datasets and sampling strategy are described in Subsection 5.1. On each of these datasets, we apply 3 different classifiers over the entire training set to estimate the optimal classification performance, the original AL framework as the baseline reference and the proposed method using G-SMOTE as a generator, described in Subsection 5.2. The metrics used to estimate the performance of these algorithms are described in Subsection 5.3. Finally, the experimental procedure is described in Subsection 5.4.

Our methodology focuses on two objectives: (1) Comparison of optimal classification performance among active learners and traditional supervised learning and (2) Comparison of classification convergence efficiency among AL frameworks.

### 5.1. Datasets

The datasets used were extracted from publicly available repositories containing hyperspectral images and ground truth data. Additionally, all datasets were collected using the same sampling procedure. The description of the hyperspectral scenes used in this study is provided in Table 2. These scenes were chosen because of their popularity in the research community and their high baseline classification scores. Consequently, demonstrating an outperforming method in this context is particularly challenging and valuable.

Dataset	Sensor	Location	Dimension	Bands	Res. (m)	Classes
Botswana	Hyperion	Okavango Delta	1476 x 256	145	30	14
Salinas A	AVIRIS	California, USA	86 x 83	224	3.7	6
Kennedy Space Center	AVIRIS	Florida, USA	512 x 614	176	18	16
Indian Pines	AVIRIS	NW Indiana, USA	145 x 145	220	20	16
Salinas	AVIRIS	California, USA	512 x 217	224	3.7	16
Pavia University	ROSIS	Pavia, Italy	610 x 610	103	1.3	9
Pavia Centre	ROSIS	Pavia, Italy	1096 x 1096	102	1.3	9

Table 2: Description of the hyperspectral scenes used in this experiment. The column “Res. (m)” refers to the resolution of the sensors (in meters) that captured each of the scenes.

The Indian Pines scene [52] is composed of agriculture fields in approximately two thirds of its coverage, low density buildup areas and natural perennial vegetation in the remainder of its area (see Figure 4a). The Pavia Centre and University scenes are hyperspectral, high-resolution images containing ground truth data composed of urban-related coverage (see Figures 4b and 4c). The Salinas and Salinas A scenes contain at-sensor radiance data. As subset of Salinas, the Salinas A scene contains contains the vegetables fields present in Salinas and the latter is also composed of bare soils and vineyard fields (see Figures 4d and 4e). The Botswana scene contains ground truth data composed of seasonal swamps, occasional swamps, and drier woodlands located in the

<sup>365</sup> distal portion of the Delta (see Figure 4f). The Kennedy Space Center scene contains a  
<sup>366</sup> ground truth composed of both vegetation and urban-related coverage (see Figure 4g).

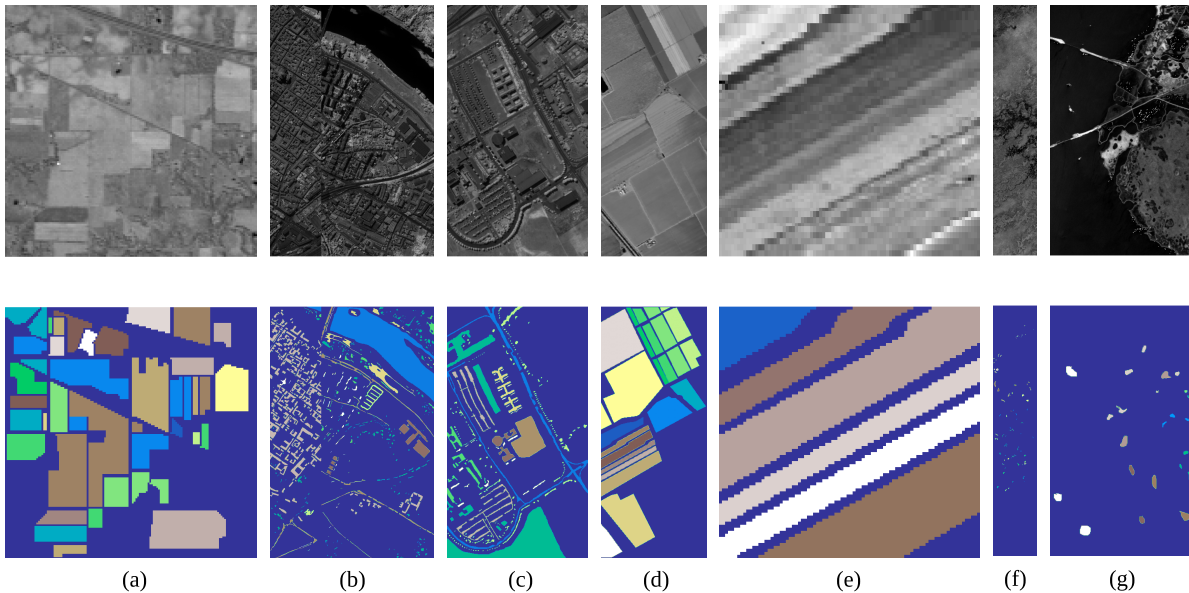


**Figure 4.** Gray scale visualization of a band (top row) and ground truth (bottom row) of each scene used in this study. (a) Indian Pines, (b) Pavia Centre, (c) Pavia University, (d) Salinas, (e) Salinas A, (f) Botswana, (g) Kennedy Space Center

<sup>367</sup> The sampling strategy is similar to all datasets. The pixels without a ground  
<sup>368</sup> truth label are first discarded. All the classes with cardinality lower than 150 are also  
<sup>369</sup> discarded. This is done to maintain feasible Imbalance Ratios (IR) across datasets  
<sup>370</sup> (where  $IR = \frac{count(C_{maj})}{count(C_{min})}$ ). Finally, a stratified sample of 1500 instances are selected for  
<sup>371</sup> the experiment. The resulting datasets are described in Table 3. The motivation for  
<sup>372</sup> this strategy is three fold: (1) reduce the datasets to a manageable size and allow the  
<sup>373</sup> experimental procedure to be completed within a feasible time frame, (2) ensure the  
<sup>374</sup> relative class frequencies in the scenes are preserved and (3) ensure equivalent analyses  
<sup>375</sup> across datasets and AL frameworks. In this context, a fixed number of instances per  
<sup>376</sup> dataset is especially important to standardize the AL-related performance metrics.

Dataset	Features	Instances	Min. Instances	Maj. Instances	IR	Classes
Botswana	145	1500	89	154	1.73	12
Salinas A	224	1500	109	428	3.93	6
Kennedy Space Center	176	1500	47	272	5.79	12
Indian Pines	220	1500	31	366	11.81	12
Salinas	224	1500	25	312	12.48	16
Pavia University	103	1500	33	654	19.82	9
Pavia Centre	102	1500	27	668	24.74	9

Table 3: Description of the datasets collected from each corresponding scene. The sampling strategy is similar to all scenes.

### <sup>377</sup> 5.2. Machine Learning Algorithms

<sup>378</sup>  
<sup>379</sup> We use two different types of ML algorithms. A data generation algorithm, used  
<sup>380</sup> to form the generator, and classification algorithms, used to calculate the classification  
<sup>381</sup> uncertainties in the unlabeled dataset and predict the class labels in the validation and  
<sup>382</sup> test sets.

383        Although any method capable of generating artificial data can be used as a generator,  
 384        the one used in this experiment is an oversampler, originally developed to deal with  
 385        imbalanced learning problems. Specifically, we chose G-SMOTE, a state-of-the-art  
 386        oversampler.

387        Three classification algorithms are used. We use different types of classifiers to  
 388        test the framework's performance under varying situations: neighbors-based, linear  
 389        and ensemble models. The neighbors-based classifier chosen was K-nearest neighbors  
 390        (KNN) [53], a logistic regression (LR) [54] is used as the linear model and a random  
 391        forest classifier (RFC) [55] was used as the ensemble model.

392        The acquisition function is completed by testing three different selection criteria.  
 393        Random selection is used as a baseline selection criterion, whereas entropy and breaking  
 394        ties are used due to their popularity and independence of the classifier used.

### 395        5.3. Evaluation Metrics

396        Since the datasets used in this experiment have an imbalanced distribution of  
 397        class frequencies, metrics such as the *Overall Accuracy* (OA) and *Kappa coefficient* are  
 398        insufficient to accurately depict classification performance [56,57]. Instead, metrics such  
 399        as Producer's Accuracy (or *Recall*) and User's Accuracy (or *Precision*) can be used. Since  
 400        they consist of ratios based on True/False Positives (TP and FP) and Negatives (TN  
 401        and FN), they provide per class information regarding the classifier's classification  
 402        performance. However, in this experiment, the meaning and number of classes available  
 403        in each dataset varies, making these metrics difficult to synthesize.

404        The performance metric *Geometric mean* (G-mean) and *F-score* are less sensitive to  
 405        the data imbalance bias [58,59]. Therefore, we employ both of these scorers. G-mean  
 406        consists of the geometric mean of *Specificity* =  $\frac{TN}{TN+FP}$  and *Sensitivity* =  $\frac{TP}{TP+FN}$  (also  
 407        known as *Recall*) [59]. Both metrics are calculated in a multiclass context considering a  
 408        one-versus-all approach. For multiclass problems, the *G-mean* scorer is calculated as its  
 409        average per class values:

$$G\text{-mean} = \sqrt{Sensitivity_i \times Specificity_i}$$

410        The F-score performance metric is the harmonic mean of *Precision* and *Recall*. The  
 411        two metrics are also calculated considering a one-versus-all approach. The *F-score* for  
 412        the multi-class case can be calculated using its average per class values [60]:

$$F\text{-score} = 2 \frac{\overline{Precision} \times \overline{Recall}}{\overline{Precision} + \overline{Recall}}$$

413        The comparison of classification convergence across AL frameworks and selection  
 414        criteria is done using 2 AL-specific performance metrics. Particularly, we follow the  
 415        recommendations found in [22]. Each AL configuration is evaluated using the *Area  
 416        Under the Learning Curve* (AULC) performance metric. It is the sum of the classification  
 417        performance values of all iterations. To facilitate the analysis of the results, we fix the  
 418        range of this metric between [0, 1] by dividing it with the total amount of iterations (*i.e.*,  
 419        the maximum performance area).

420        The *Data Utilization Rate* (DUR) [61] metric consists of the ratio between the number  
 421        of instances required to reach a given G-mean score threshold by an AL strategy and  
 422        an equivalent baseline strategy. For easier interpretability, we simplify this metric by  
 423        using the percentage of training data used by an AL strategy to reach the performance  
 424        threshold, instead of presenting these values as a ratio of the baseline strategy. The DUR  
 425        metric is measured at 9 different performance levels, between 0.6 and 0.95 G-mean scores  
 426        at a 0.05 step.

### 427        5.4. Experimental Procedure

430 A common practice in methodological evaluations is the implementation of an  
 431 offline experiment [62]. It consists of using an existing set of labeled data as a proxy for  
 432 the population of unlabeled instances. Because the dataset is already fully labeled, the  
 433 supervisor's typical annotation process involved in each iteration is done at zero cost.  
 434 Each AL and classifier configuration is tested using a stratified 5-fold cross validation  
 435 testing scheme. For each round, the larger partition is split in a stratified fashion to form a  
 436 training and validation set (containing 20% of the original partition). The validation set is  
 437 used to evaluate the convergence efficiency of active learners; the chooser's classification  
 438 performance metrics and amount of data points used at each iteration are used to  
 439 compute the AULC and DUR. Additionally, within the AL iterative process, the classifier  
 440 with optimal performance on the validation set is evaluated using the test set. In  
 441 order to further reduce possible initialization biases, this procedure is repeated 3 times  
 442 with different initialization seeds and the results of all runs are averaged (*i.e.*, each  
 443 configuration is trained and evaluated 15 times). Finally, the maximum performance  
 444 lines are calculated using the same approach. In those cases, the validation set is not  
 445 used. The experimental procedure is depicted in Figure 5.

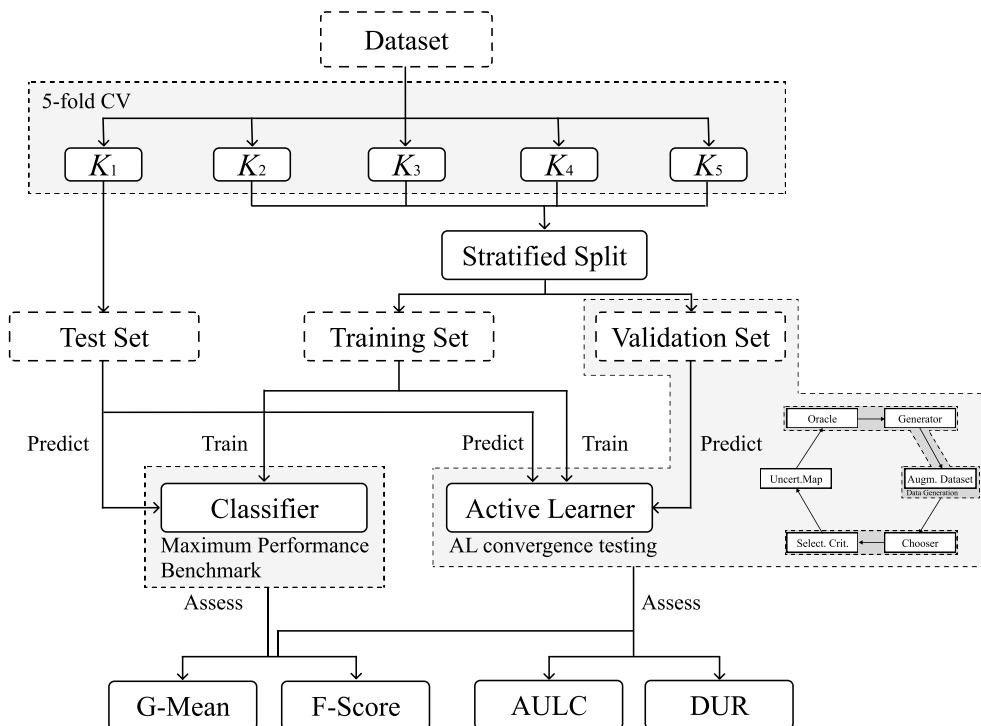


**Figure 5.** Experimental procedure. The datasets extracted from hyperspectral scenes are split in 5 folds. 1 of those (*e.g.*,  $K_1$ ) is used to test the optimal performance of AL algorithms and the classification without AL. The training set is used to iterate AL algorithms and train classifiers. The validation set is used to test the convergence of AL algorithms. The results are averaged over the 5 folds across each of the 3 different initializations of this procedure.

446 To make the AL-specific metrics comparable among active learners, the configura-  
 447 tions of the different frameworks must be similar. For each dataset, the number of  
 448 instances is constant to facilitate the analysis of the same metrics.

449 In most practical AL applications it is assumed that the number of instances in the  
 450 initial training sample is too small to perform hyperparameter tuning. Consequently,  
 451 in order to ensure realistic results, our experimental procedure does not include hyper-  
 452 parameter optimization. The predefined hyperparameters are shown in Table 4. They  
 453 were set up based on general recommendations and default settings for the classifiers  
 454 and generators used.

<sup>455</sup> The AL iterative process is set up with a randomly selected initial training sample  
<sup>456</sup> with 15 initial samples. At each iteration, 15 additional samples are added to the training  
<sup>457</sup> set. This process is stopped after 49 iterations, once 50% of the entire dataset (*i.e.*, 78% of  
<sup>458</sup> the training set) is added to the augmented dataset.

Classifier	Hyperparameters	Values
LR	maximum iterations	10000
	solver	sag
	penalty	None
KNN	# neighbors	5
	weights	uniform
	metric	euclidean
RF	maximum tree depth	None
	# estimators	100
	criterion	gini
<hr/>		
Generator		
G-SMOTE	# neighbors	5
	deformation factor	0.5
	truncation factor	0.5

Table 4: Hyper-parameter definition for the classifiers and generator used in the experiment.

<sup>459</sup> *5.5. Software Implementation*

<sup>460</sup> The experiment was implemented using the Python programming language, along  
<sup>461</sup> with the Python libraries [Scikit-Learn](#) [63], [Imbalanced-Learn](#) [64], [Geometric-SMOTE](#),  
<sup>462</sup> [Cluster-Over-Sampling](#) and [Research-Learn](#) libraries. All functions, algorithms, experi-  
<sup>463</sup> ments and results are provided in the [GitHub repository of the project](#).

<sup>464</sup> **6. Results & Discussion**

<sup>465</sup>

<sup>466</sup> The evaluation of the different AL frameworks in a multiple dataset context should  
<sup>467</sup> not rely uniquely on the mean of the performance metrics across datasets. [65] recom-  
<sup>468</sup> mends the use of mean ranking scores, since the performance levels of the different  
<sup>469</sup> frameworks varies according to the data it is being used on. Consequently, evaluating  
<sup>470</sup> these performance metrics solely based on their mean values might lead to inaccurate  
<sup>471</sup> analyses. Accordingly, the results of this experiment are analysed using both the mean  
<sup>472</sup> ranking and absolute scores for each model. The rank values are assigned based on the  
<sup>473</sup> mean scores resulting from three different initializations of 5-fold cross validation for  
<sup>474</sup> each classifier and active learner. The goal of this analysis is to understand whether the  
<sup>475</sup> proposed framework (AL with the integration of an artificial data generator) is capable  
<sup>476</sup> of using less data from the original dataset while simultaneously achieving better classi-  
<sup>477</sup> fication results than the standard AL framework, *i.e.*, guarantee a faster classification  
<sup>478</sup> convergence.

<sup>479</sup> *6.1. Results*

<sup>480</sup>

<sup>481</sup> Table 5 shows the average rankings and standard deviations across datasets of the  
<sup>482</sup> AULC scores for each active learner.

Classifier	Evaluation Metric	Standard	Proposed
KNN	F-score	$2.00 \pm 0.0$	<b><math>1.00 \pm 0.0</math></b>
KNN	G-mean	$2.00 \pm 0.0$	<b><math>1.00 \pm 0.0</math></b>
LR	F-score	$1.71 \pm 0.45$	<b><math>1.29 \pm 0.45</math></b>
LR	G-mean	$2.00 \pm 0.0$	<b><math>1.00 \pm 0.0</math></b>
RF	F-score	$1.86 \pm 0.35$	<b><math>1.14 \pm 0.35</math></b>
RF	G-mean	$2.00 \pm 0.0$	<b><math>1.00 \pm 0.0</math></b>

Table 5: Mean rankings of the AULC metric over the different datasets (7), folds (5) and runs (3) used in the experiment. This means that the use of G-SMOTE almost always improves the results of the original framework.

483        The mean AULC absolute scores are provided in Table 6. These values are computed  
 484        as the mean of the sum of the scores of a specific performance metric over all iterations  
 485        (for an AL configuration). In other words, these values correspond to the average AULC  
 486        over 7 datasets  $\times$  5 folds  $\times$  3 initializations.

Classifier	Evaluation Metric	Standard	Proposed
KNN	F-score	$0.762 \pm 0.131$	<b><math>0.794 \pm 0.123</math></b>
KNN	G-mean	$0.864 \pm 0.079$	<b><math>0.886 \pm 0.073</math></b>
LR	F-score	$0.839 \pm 0.119$	<b><math>0.843 \pm 0.116</math></b>
LR	G-mean	$0.907 \pm 0.074$	<b><math>0.911 \pm 0.071</math></b>
RF	F-score	$0.810 \pm 0.109$	<b><math>0.819 \pm 0.1</math></b>
RF	G-mean	$0.890 \pm 0.068$	<b><math>0.901 \pm 0.059</math></b>

Table 6: Average AULC of each AL configuration tested. Each AULC score is calculated using the G-mean scores of each iteration in the validation set. By the end of the iterative process, each AL configuration used a total of 750 instances of the 960 instances that compose the training set.

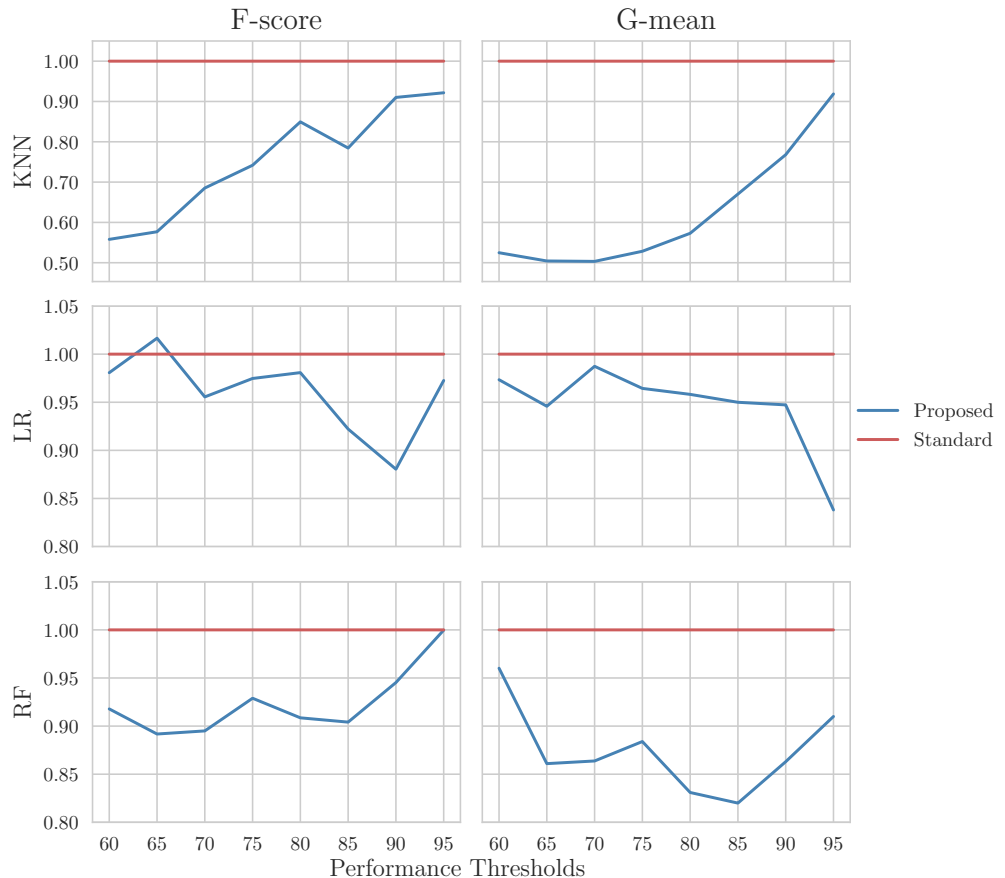
487        The average DURs are shown in Table 4. They were calculated for various G-mean  
 488        scores thresholds, varying at a step of 5% between 60% and 95%. Each row shows the  
 489        percentage of training data required by the different AL configurations to reach that  
 490        specific G-mean score.

G-mean Score	Classifier	Standard	Proposed
0.60	KNN	4.0%	<b>2.1%</b>
0.60	LR	2.2%	<b>2.1%</b>
0.60	RF	2.2%	<b>2.1%</b>
0.65	KNN	5.6%	<b>2.8%</b>
0.65	LR	3.0%	<b>2.7%</b>
0.65	RF	3.1%	<b>2.6%</b>
0.70	KNN	7.9%	<b>4.1%</b>
0.70	LR	4.2%	<b>4.1%</b>
0.70	RF	4.5%	<b>3.6%</b>
0.75	KNN	13.5%	<b>7.1%</b>
0.75	LR	7.2%	<b>6.6%</b>
0.75	RF	6.6%	<b>5.4%</b>
0.80	KNN	24.4%	<b>16.9%</b>
0.80	LR	13.1%	<b>11.7%</b>
0.80	RF	11.6%	<b>9.2%</b>
0.85	KNN	29.8%	<b>23.6%</b>
0.85	LR	19.8%	<b>18.8%</b>
0.85	RF	23.1%	<b>17.3%</b>

G-mean Score	Classifier	Standard	Proposed
0.90	KNN	41.0%	<b>36.1%</b>
0.90	LR	28.1%	<b>24.8%</b>
0.90	RF	37.1%	<b>30.3%</b>
0.95	KNN	71.3%	<b>69.1%</b>
0.95	LR	45.8%	<b>40.2%</b>
0.95	RF	64.6%	<b>62.2%</b>

Table 4: Mean data utilization of AL algorithms, as a percentage of the training set.

491 The DUR of the proposed method relative to the baseline method is shown in  
 492 Figure 6. A DUR below 1 means that the proposed framework requires less data to reach  
 493 the same performance threshold (as a percentage, relative to the amount of data required  
 494 by the baseline framework). For instance, in the upper left graphic we can see that the  
 495 proposed framework achieves 90% classification using F-score while using 91% of the  
 496 amount of data used by the traditional AL framework, in other words 9% less data.

**Figure 6.** Mean data utilization rates. The y-axis shows the percentage of data (relative to the baseline AL framework) required to reach the different performance thresholds.

497 The averaged optimal classification scores are shown in Table 5. The maximum  
 498 performance (MP) classification scores are shown as a benchmark and represent the  
 499 performance of the corresponding classifier using the entire training set.

Classifier	Evaluation Metric	MP	Standard	Proposed
KNN	F-score	0.838 ± 0.106	0.835 ± 0.115	<b>0.843 ± 0.105</b>
KNN	G-mean	0.907 ± 0.063	0.904 ± 0.069	<b>0.912 ± 0.061</b>
LR	F-score	<b>0.890 ± 0.084</b>	0.883 ± 0.096	0.887 ± 0.097
LR	G-mean	0.935 ± 0.052	0.931 ± 0.059	<b>0.938 ± 0.055</b>
RF	F-score	0.859 ± 0.083	0.866 ± 0.081	<b>0.869 ± 0.08</b>
RF	G-mean	0.918 ± 0.051	0.921 ± 0.051	<b>0.930 ± 0.043</b>

Table 5: Optimal classification scores. The Maximum Performance (MP) classification scores are calculated using classifiers trained using the entire training set.

### 500 6.2. Statistical Analysis

501  
 502 The methods used to test the experiment's results must be appropriate for a multi-  
 503 dataset context. Therefore the statistical analysis is performed using the Wilcoxon signed-  
 504 rank test [66] as a post-hoc analysis. The variable used for this test is the data utilization  
 505 rate based on the G-mean performance metric, considering the various performance  
 506 thresholds from Table 4.

507 The Wilcoxon signed-rank test results are shown in Table 6. We test as null hypoth-  
 508 esis that the performance of the proposed framework is the same as the original AL  
 509 framework. The null hypothesis was rejected in all datasets.

Dataset	p-value	Significance
Botswana	3.8e-03	True
Indian Pines	2.3e-04	True
Kennedy Space Center	1.3e-04	True
Pavia Centre	4.3e-03	True
Pavia University	4.6e-05	True
Salinas	4.6e-05	True
Salinas A	3.0e-03	True

Table 6: Adjusted p-values using the Wilcoxon signed-rank method. Bold values are statistically significant at a level of  $\alpha = 0.05$ . The null hypothesis is that the performance of the proposed framework is similar to that of the original framework.

### 510 6.3. Discussion

511 This paper expands the AL framework by adding an artificial data generator into its  
 512 iterative process. This modification is done to accelerate the classification convergence  
 513 of the standard AL procedure, which is reflected in the reduction of the amount of data  
 514 necessary to reach better classification results.

515 The convergence efficiency of the proposed method is always higher than the  
 516 baseline AL framework, with the exception of one comparison, as shown in Table 5 and  
 517 Figure 6. This means the proposed AL framework using data generation was able to  
 518 outperform the baseline AL in nearly all scenarios.

519 The mean AUC scores in Table 6 show a significant improvement in the per-  
 520 formance of AL when a generator is used. The mean performance of the proposed  
 521 framework is always better than the baseline framework. This improvement is explained  
 522 by:

- 523 1. Earlier convergence of AL, *i.e.*, requiring less data to achieve comparable perfor-  
 524 mance levels. This effect is shown in Table 4, where we found that the proposed  
 525 framework always uses less data for similar performance levels, regardless of the  
 526 classifier used.

527 2. Higher optimal classification performance, *i.e.*, reaching higher performance levels  
528 overall. This effect is shown in Table 5, where we found that using a generator in  
529 AL led to a better classification performance and was capable of outperforming the  
530 MP threshold.

531 Our results show statistical significance in every dataset. The proposed framework  
532 had a superior performance with statistical significance on each dataset at a level of  
533  $\alpha = 0.05$ . This indicates that regardless of the context under which an AL algorithm is  
534 used, the proposed framework reduces the amount of data necessary in the AL's iterative  
535 process.

536 This paper introduces the concept of applying data a generation algorithm in the  
537 AL framework. This was done with the implementation of a recent state of the art  
538 generalization of a popular data generation algorithm. Although, since this algorithm  
539 is based on heuristics, future work should focus on improving these results through  
540 the design of new data generation mechanisms, at the cost of additional computational  
541 power. In addition, we also noticed significant standard errors in our experimental  
542 results (see Subsection 6.1). This indicates that AL procedures seem to be particularly  
543 sensitive to the initialization method, which is still a limitation of AL, regardless of the  
544 framework and configurations used. This is consistent with the findings in [22], which  
545 future work should attempt to address. Although using a generator marginally reduced  
546 this standard error, it is not sufficient to address this specific limitation.

## 547 7. Conclusion

548 The aim of this experiment was to test the effectiveness of a new AL framework  
549 that introduces artificial data generation in its iterative process. The experiment was  
550 designed to test the proposed method under particularly challenging conditions, where  
551 the maximum performance line is naturally high in most datasets. The element that  
552 constitute the Generator component was set up in a plug-and-play scheme, without  
553 significant tuning of the G-SMOTE oversampler. Using a generator in AL improved  
554 the original AL framework in all scenarios. These results could be further improved  
555 through the modification and more intense tuning of the data generation strategy. In  
556 our experiment, artificial data was generated only to match each non-majority class  
557 frequency with the majority class frequency, strictly balancing the class distribution.  
558 Generating a larger amount of data for all classes can further improve these results.

559 The high performance scores for the baseline AL framework made the achievement  
560 of significant improvements over the traditional AL framework under these conditions  
561 particularly meaningful. The advantage of the proposed AL framework is shown in  
562 Table 4. In most of the presented scenarios there is a substantial reduction of data  
563 necessary to reach a given performance threshold.

564 The results from this experiment show that using a data generator in the AL frame-  
565 work will improve the convergence of the method. This framework successfully antici-  
566 pate the predictor's optimal performance, as shown in Tables 5, 6 and 4. Therefore, in a  
567 real application, the annotation cost would have been reduced since less iterations and  
568 labeled instances are necessary to reach near optimal classification performance.

569 **Acknowledgments:** The authors would like to thank Professor Victor Lobo (NOVA IMS, Universi-  
570 dade Nova de Lisboa, and CINAV, Escola Naval, CIDIUM) for reviewing this paper and providing  
571 important feedback throughout its development.

572 **Author Contributions:** Conceptualization, F.B.; Methodology, J.F. and G.D.; Software, J.F. and  
573 G.D.; Validation, F.B., G.D.; Formal Analysis, J.F.; Writing - Original Draft Preparation, J.F.; Writing  
574 - Review & Editing, F.B., G.D., J.F.; Supervision, F.B.; Funding Acquisition, F.B.

575 **Funding:** This research was funded by “Fundação para a Ciência e a Tecnologia” (Portugal)  
576 [grant numbers PCIF/SSI/0102/2017 - foRESTER, DSAIPA/AI/0100/2018 - IPSTERS].

**578 Data Availability Statement:** The data reported in this study is publicly available. It can  
579 be retrieved and preprocessed using the Python source code provided at <https://github.com/joaopfonseca/research>. Alternatively the original data is available at [http://www.ehu.eus/ccwintco/index.php?title=Hyperspectral\\_Remote\\_Sensing\\_Scenes](http://www.ehu.eus/ccwintco/index.php?title=Hyperspectral_Remote_Sensing_Scenes).

**582 Conflicts of Interest:** The authors declare no conflict of interest. The funders had no role in the  
583 design of the study; in the collection, analyses, or interpretation of data; in the writing of the  
584 manuscript, or in the decision to publish the results.

## References

1. Nagai, S.; Nasahara, K.N.; Akitsu, T.K.; Saitoh, T.M.; Muraoka, H. Importance of the Collection of Abundant Ground-Truth Data for Accurate Detection of Spatial and Temporal Variability of Vegetation by Satellite Remote Sensing. In *Biogeochemical Cycles: Ecological Drivers and Environmental Impact*; American Geophysical Union (AGU), 2020; pp. 223–244. doi:10.1002/9781119413332.ch11.
2. Huang, Y.; xin CHEN, Z.; YU, T.; zhi HUANG, X.; fa GU, X. Agricultural remote sensing big data: Management and applications. *Journal of Integrative Agriculture* **2018**, *17*, 1915–1931. doi:10.1016/S2095-3119(17)61859-8.
3. Wang, X.; Xie, H. A review on applications of remote sensing and geographic information systems (GIS) in water resources and flood risk management. *Water (Switzerland)* **2018**, *10*, 608. doi:10.3390/w10050608.
4. Khatami, R.; Mountrakis, G.; Stehman, S.V. A meta-analysis of remote sensing research on supervised pixel-based land-cover image classification processes: General guidelines for practitioners and future research. *Remote Sensing of Environment* **2016**, *177*, 89–100. doi:10.1016/J.RSE.2016.02.028.
5. Gavade, A.B.; Rajpurohit, V.S. Systematic analysis of satellite image-based land cover classification techniques: literature review and challenges. *International Journal of Computers and Applications* **2019**, pp. 1–10. doi:10.1080/1206212x.2019.1573946.
6. Wulder, M.A.; Coops, N.C.; Roy, D.P.; White, J.C.; Hermosilla, T. Land cover 2.0. *International Journal of Remote Sensing* **2018**, *39*, 4254–4284. doi:10.1080/01431161.2018.1452075.
7. Costa, H.; Benevides, P.; Marcelino, F.; Caetano, M. Introducing automatic satellite image processing into land cover mapping by photo-interpretation of airborne data. *The International Archives of Photogrammetry, Remote Sensing and Spatial Information Sciences* **2020**, *42*, 29–34.
8. Vermote, E.F.; Skakun, S.; Becker-Reshef, I.; Saito, K. Remote Sensing of Coconut Trees in Tonga Using Very High Spatial Resolution WorldView-3 Data. *Remote Sensing* **2020**, *12*, 3113.
9. Costantino, D.; Pepe, M.; Dardanelli, G.; Baiocchi, V. USING OPTICAL SATELLITE AND AERIAL IMAGERY FOR AUTOMATIC COASTLINE MAPPING. *Geographia Technica* **2020**, pp. 171–190. doi:10.21163/gt\_2020.152.17.
10. Maxwell, A.E.; Warner, T.A.; Fang, F. Implementation of machine-learning classification in remote sensing: An applied review. *International Journal of Remote Sensing* **2018**, *39*, 2784–2817. doi:10.1080/01431161.2018.1433343.
11. Růžička, V.; D'Aronco, S.; Wegner, J.D.; Schindler, K. Deep Active Learning in Remote Sensing for data efficient Change Detection. *arXiv preprint arXiv:2008.11201* **2020**.
12. Liu, S.J.; Luo, H.; Shi, Q. Active Ensemble Deep Learning for Polarimetric Synthetic Aperture Radar Image Classification. *IEEE Geoscience and Remote Sensing Letters* **2020**, pp. 1–5, [2006.15771]. doi:10.1109/lgrs.2020.3005076.
13. Su, T.; Zhang, S.; Liu, T. Multi-spectral image classification based on an object-based active learning approach. *Remote Sensing* **2020**, *12*, 504. doi:10.3390/rs12030504.
14. Pasolli, E.; Yang, H.L.; Crawford, M.M. Active-metric learning for classification of remotely sensed hyperspectral images. *IEEE Transactions on Geoscience and Remote Sensing* **2016**, *54*, 1925–1939. doi:10.1109/TGRS.2015.2490482.
15. Pelletier, C.; Valero, S.; Ingla, J.; Champion, N.; Sicre, C.M.; Dedieu, G. Effect of training class label noise on classification performances for land cover mapping with satellite image time series. *Remote Sensing* **2017**, *9*, 173. doi:10.3390/rs9020173.
16. Stromann, O.; Nascenti, A.; Yousif, O.; Ban, Y. Dimensionality Reduction and Feature Selection for Object-Based Land Cover Classification based on Sentinel-1 and Sentinel-2 Time Series Using Google Earth Engine. *Remote Sensing* **2020**, *12*, 76. doi:10.3390/RS12010076.
17. Alonso-Sarria, F.; Valdivieso-Ros, C.; Gomariz-Castillo, F. Isolation forests to evaluate class separability and the representativeness of training and validation areas in land cover classification. *Remote Sensing* **2019**, *11*, 3000. doi:10.3390/rs11243000.
18. Feng, W.; Huang, W.; Ye, H.; Zhao, L. Synthetic minority over-sampling technique based rotation forest for the classification of unbalanced hyperspectral data. International Geoscience and Remote Sensing Symposium (IGARSS). Institute of Electrical and Electronics Engineers Inc., 2018, Vol. 2018-July, pp. 2651–2654. doi:10.1109/IGARSS.2018.8518242.
19. Chawla, N.V.; Japkowicz, N.; Kotcz, A. Editorial: Special Issue on Learning from Imbalanced Data Sets. *ACM SIGKDD Explorations Newsletter* **2004**, *6*, 1–6. doi:10.1145/1007730.1007733.
20. Fernández, A.; López, V.; Galar, M.; del Jesus, M.J.; Herrera, F. Analysing the classification of imbalanced data-sets with multiple classes: Binarization techniques and ad-hoc approaches. *Knowledge-Based Systems* **2013**, *42*, 97–110. doi:10.1016/J.KNOSYS.2013.01.018.
21. Kaur, H.; Pannu, H.S.; Malhi, A.K. A systematic review on imbalanced data challenges in machine learning: Applications and solutions. *ACM Computing Surveys* **2019**, *52*, 1–36. doi:10.1145/3343440.
22. Kottke, D.; Calma, A.; Huseljic, D.; Kreml, G.; Sick, B. Challenges of reliable, realistic and comparable active learning evaluation. CEUR Workshop Proceedings, 2017, Vol. 1924, pp. 2–14.

23. Sverchkov, Y.; Craven, M. A review of active learning approaches to experimental design for uncovering biological networks. *PLOS Computational Biology* **2017**, *13*, e1005466. doi:10.1371/journal.pcbi.1005466.
24. Li, J.; Huang, X.; Chang, X. A label-noise robust active learning sample collection method for multi-temporal urban land-cover classification and change analysis. *ISPRS Journal of Photogrammetry and Remote Sensing* **2020**, *163*, 1–17. doi:10.1016/j.isprsjprs.2020.02.022.
25. Yoo, D.; Kweon, I.S. Learning Loss for Active Learning. Proceedings of the IEEE/CVF Conference on Computer Vision and Pattern Recognition (CVPR), 2019.
26. Aghdam, H.H.; Gonzalez-Garcia, A.; Lopez, A.; Weijer, J. Active learning for deep detection neural networks. Proceedings of the IEEE International Conference on Computer Vision, 2019, Vol. 2019-Octob, pp. 3671–3679, [1911.09168]. doi:10.1109/ICCV.2019.00377.
27. Cawley, G. Baseline Methods for Active Learning. *Proceedings of Active Learning and Experimental Design workshop In conjunction with AISTATS* **2011**, *16*, 47–57.
28. Li, X.; Guo, Y. Active learning with multi-label SVM classification. In IJCAI, 2013, pp. 1479–1485.
29. Tuia, D.; Pasolli, E.; Emery, W.J. Using active learning to adapt remote sensing image classifiers. *Remote Sensing of Environment* **2011**, *115*, 2232–2242.
30. Cao, X.; Yao, J.; Xu, Z.; Meng, D. Hyperspectral Image Classification with Convolutional Neural Network and Active Learning. *IEEE Transactions on Geoscience and Remote Sensing* **2020**, *58*, 4604–4616. doi:10.1109/TGRS.2020.2964627.
31. Wu, X.; Li, W.; Hong, D.; Tian, J.; Tao, R.; Du, Q. Vehicle detection of multi-source remote sensing data using active fine-tuning network. *ISPRS Journal of Photogrammetry and Remote Sensing* **2020**, *167*, 39–53, [2007.08494]. doi:10.1016/j.isprsjprs.2020.06.016.
32. Bi, H.; Xu, F.; Wei, Z.; Xue, Y.; Xu, Z. An Active Deep Learning Approach for Minimally Supervised PolSAR Image Classification. *IEEE Transactions on Geoscience and Remote Sensing* **2019**, *57*, 9378–9395. doi:10.1109/TGRS.2019.2926434.
33. Shrivastava, V.K.; Pradhan, M.K. Hyperspectral Remote Sensing Image Classification Using Active Learning. In *Studies in Computational Intelligence*; Springer, 2021; Vol. 907, pp. 133–152. doi:10.1007/978-3-030-50641-4\_8.
34. Muslea, I.; Minton, S.; Knoblock, C.A. Active learning with multiple views. *Journal of Artificial Intelligence Research* **2006**, *27*, 203–233, [1110.1073]. doi:10.1613/jair.2005.
35. Di, W.; Crawford, M.M. View generation for multiview maximum disagreement based active learning for hyperspectral image classification. *IEEE Transactions on Geoscience and Remote Sensing* **2012**, *50*, 1942–1954. doi:10.1109/TGRS.2011.2168566.
36. Zhou, X.; Prasad, S.; Crawford, M. Wavelet domain multi-view active learning for hyperspectral image analysis. Workshop on Hyperspectral Image and Signal Processing, Evolution in Remote Sensing. IEEE Computer Society, 2014, Vol. 2014-June. doi:10.1109/WHISPERS.2014.8077528.
37. Zhang, Z.; Pasolli, E.; Yang, H.L.; Crawford, M.M. Multimetric Active Learning for Classification of Remote Sensing Data. *IEEE Geoscience and Remote Sensing Letters* **2016**, *13*, 1007–1011. doi:10.1109/LGRS.2016.2560623.
38. Tuia, D.; Ratle, F.; Pacifici, F.; Kanevski, M.F.; Emery, W.J. Active learning methods for remote sensing image classification. *IEEE Transactions on Geoscience and Remote Sensing* **2009**, *47*, 2218–2232. doi:10.1109/TGRS.2008.2010404.
39. Copo, L.; Tuia, D.; Volpi, M.; Kanevski, M. Unbiased query-by-bagging active learning for VHR image classification. Image and Signal Processing for Remote Sensing XVI; Bruzzone, L., Ed. SPIE, 2010, Vol. 7830, p. 78300K. doi:10.1117/12.864861.
40. Demir, B.; Persello, C.; Bruzzone, L. Batch-mode active-learning methods for the interactive classification of remote sensing images. *IEEE Transactions on Geoscience and Remote Sensing* **2011**, *49*, 1014–1031. doi:10.1109/TGRS.2010.2072929.
41. Li, J.; Bioucas-Dias, J.M.; Plaza, A. Hyperspectral image segmentation using a new bayesian approach with active learning. *IEEE Transactions on Geoscience and Remote Sensing* **2011**, *49*, 3947–3960. doi:10.1109/TGRS.2011.2128330.
42. Liu, W.; Yang, J.; Li, P.; Han, Y.; Zhao, J.; Shi, H. A novel object-based supervised classification method with active learning and random forest for PolSAR imagery. *Remote Sensing* **2018**, *10*. doi:10.3390/rs10071092.
43. Luo, T.; Kramer, K.; Goldgof, D.; Hall, L.O.; Samson, S.; Remsen, A.; Hopkins, T. Learning to recognize plankton. Proceedings of the IEEE International Conference on Systems, Man and Cybernetics, 2003, Vol. 1, pp. 888–893. doi:10.1109/icsmc.2003.1243927.
44. Li, J.; Bioucas-Dias, J.M.; Plaza, A. Spectral-spatial classification of hyperspectral data using loopy belief propagation and active learning. *IEEE Transactions on Geoscience and Remote Sensing* **2013**, *51*, 844–856. doi:10.1109/TGRS.2012.2205263.
45. Ertekin, S.; Huang, J.; Giles, C.L. Active learning for class imbalance problem. Proceedings of the 30th Annual International ACM SIGIR Conference on Research and Development in Information Retrieval, SIGIR'07; ACM Press: New York, New York, USA, 2007; pp. 823–824. doi:10.1145/1277741.1277927.
46. DeVries, T.; Taylor, G.W. Dataset augmentation in feature space. 5th International Conference on Learning Representations, ICLR 2017 - Workshop Track Proceedings. International Conference on Learning Representations, ICLR, 2017, [1702.05538].
47. Chawla, N.V.; Bowyer, K.W.; Hall, L.O.; Kegelmeyer, W.P. SMOTE: Synthetic minority over-sampling technique. *Journal of Artificial Intelligence Research* **2002**, *16*, 321–357, [1106.1813]. doi:10.1613/jair.953.
48. Jozdani, S.E.; Johnson, B.A.; Chen, D. Comparing Deep Neural Networks, Ensemble Classifiers, and Support Vector Machine Algorithms for Object-Based Urban Land Use/Land Cover Classification. *Remote Sensing* **2019**, *11*, 1713. doi:10.3390/rs11141713.
49. Bogner, C.; Seo, B.; Rohner, D.; Reineking, B. Classification of rare land cover types: Distinguishing annual and perennial crops in an agricultural catchment in South Korea. *PLoS ONE* **2018**, *13*. doi:10.1371/journal.pone.0190476.
50. Douzas, G.; Bacao, F. Geometric SMOTE a geometrically enhanced drop-in replacement for SMOTE. *Information Sciences* **2019**, *501*, 118–135. doi:10.1016/j.ins.2019.06.007.

51. Douzas, G.; Bacao, F.; Fonseca, J.; Khudinyan, M. Imbalanced learning in land cover classification: Improving minority classes' prediction accuracy using the geometric SMOTE algorithm. *Remote Sensing* **2019**, *11*, 3040. doi:10.3390/rs11243040.
52. Baumgardner, M.F.; Biehl, L.L.; Landgrebe, D.A. 220 Band AVIRIS Hyperspectral Image Data Set: June 12, 1992 Indian Pine Test Site 3, 2015. doi:doi:/10.4231/R7RX991C.
53. Cover, T.; Hart, P. Nearest neighbor pattern classification. *IEEE Transactions on Information Theory* **1967**, *13*, 21–27. doi:10.1109/TIT.1967.1053964.
54. Nelder, J.A.; Wedderburn, R.W. Generalized linear models. *Journal of the Royal Statistical Society: Series A (General)* **1972**, *135*, 370–384.
55. Ho, T.K. Random Decision Forests. Proceedings of the Third International Conference on Document Analysis and Recognition (Volume 1) - Volume 1; IEEE Computer Society: USA, 1995; ICDAR '95, p. 278.
56. Olofsson, P.; Foody, G.M.; Stehman, S.V.; Woodcock, C.E. Making better use of accuracy data in land change studies: Estimating accuracy and area and quantifying uncertainty using stratified estimation. *Remote Sensing of Environment* **2013**, *129*, 122–131. doi:10.1016/j.rse.2012.10.031.
57. Pontius, R.G.; Millones, M. Death to Kappa: Birth of quantity disagreement and allocation disagreement for accuracy assessment. *International Journal of Remote Sensing* **2011**, *32*, 4407–4429. doi:10.1080/01431161.2011.552923.
58. Jeni, L.A.; Cohn, J.F.; De La Torre, F. Facing imbalanced data - Recommendations for the use of performance metrics. Proceedings - 2013 Humaine Association Conference on Affective Computing and Intelligent Interaction, ACII 2013, 2013, pp. 245–251. doi:10.1109/ACII.2013.47.
59. Kubat, M.; Matwin, S.; others. Addressing the curse of imbalanced training sets: one-sided selection. Icm. Citeseer, 1997, Vol. 97, pp. 179–186.
60. He, H.; Garcia, E.A. Learning from Imbalanced Data. *IEEE Transactions on Knowledge and Data Engineering* **2009**, *21*, 1263–1284, [arXiv:1011.1669v3]. doi:10.1109/TKDE.2008.239.
61. Reitmaier, T.; Sick, B. Let us know your decision: Pool-based active training of a generative classifier with the selection strategy 4DS. *Information Sciences* **2013**, *230*, 106–131.
62. Kagy, J.F.; Kayadelen, T.; Ma, J.; Rostamizadeh, A.; Strnadova, J. The Practical Challenges of Active Learning: Lessons Learned from Live Experimentation, 2019, [arXiv:cs.LG/1907.00038].
63. Pedregosa, F.; Varoquaux, G.; Gramfort, A.; Michel, V.; Thirion, B.; Grisel, O.; Blondel, M.; Prettenhofer, P.; Weiss, R.; Dubourg, V.; Vanderplas, J.; Passos, A.; Cournapeau, D.; Brucher, M.; Perrot, M.; Duchesnay, É. Scikit-learn: Machine Learning in Python. *Journal of Machine Learning Research* **2011**, *12*, 2825–2830.
64. Lemaître, G.; Nogueira, F.; Aridas, C.K. Imbalanced-learn: A Python Toolbox to Tackle the Curse of Imbalanced Datasets in Machine Learning. *Journal of Machine Learning Research* **2017**, *18*, 1–5.
65. Demšar, J. Statistical comparisons of classifiers over multiple data sets. *Journal of Machine learning research* **2006**, *7*, 1–30.
66. Wilcoxon, F. Individual Comparisons by Ranking Methods. *Biometrics Bulletin* **1945**, *1*, 80. doi:10.2307/3001968.